Sigma J Eng Nat Sci, Vol. 43, No. 4, pp. 1140–1151, August, 2025

Sigma Journal of Engineering and Natural Sciences
Web page info: https://sigma.yildiz.edu.tr
DOI: 10.14744/sigma.2025.00110

Research Article

Thermo-mechanical analysis in a simply supported plate using a fractional order approach

Navneet LAMBA[1,*], Jyoti VERMA[2], Kishor DESHMUKH[3]

[1]Department of Mathematics, Shri Lemdeo Patil Mahavidyalaya, Mandhal, Nagpur, 440001, India
[2]Department of Mathematics, SVKMs Narsee Monjee Institute of Management Studies, School of Science, Navi Mumbai, 400056, India
[3]Department of Mathematics, R.T.M., Nagpur University, Nagpur, 440033, India

ARTICLE INFO

Article history
Received: 31 January 2024
Revised: 11 May 2024
Accepted: 21 July 2024

Keywords:
Fractional Order Theory; Heat Source; Rectangular Plate; Thermal Bending Moment; Thermal Stress

ABSTRACT

A simply supported rectangular plate of small thickness with a thermal bending moment is considered in this proposed work, and fractional order theory is used to analyze the thermoelastic effects. A point heat source that is instantly available and situated anywhere inside the solid rectangular plate is also present. The influences of thermally stressed components are evaluated for weak, moderate, and superconductivity using the thermal moment of bending. The outcomes are achieved as a series solution, and the corresponding convergences have been illustrated. For computational analysis, copper-based material properties of a rectangular plate shape are assumed, and graphically plotted results are presented successfully. In the above-mentioned study, we prepared the mathematical model for defined parameters and functions and illustrated the result with physical significance. Till date, only studies have shown the thermal bending moment for classical heat conduction equations, whereas this work, considered heat conduction containing a fractional order approach, which predicts the retarded response, and it also interpolates classical heat conduction equations. As a part of the comparison, the limiting case is discussed.

Cite this article as: Lamba N, Verma J, Deshmukh K. Thermo-mechanical analysis in a simply supported plate using a fractional order approach. Sigma J Eng Nat Sci 2025;43(4):1140–1151.

INTRODUCTION

In the preceding years, the requirements for using fractional calculus to describe complex phenomena, i.e., multiphysics couplings, multiscale couplings, etc., have increased dramatically. Thermoelasticity has made a lot of use of derivatives of fractions recently, and renowned researchers, mathematicians, and scientists are working hard to develop it further. The domains of practical sciences and engineering are two areas where fractional calculus is used in a variety of applications (included in the books by Podlubny [1], Atanacković et al. [2], Herrmann [3], Magin [4], Mainardi [5], West et al. [6], and Zaslavsky [7]). Povstenko performed a study on thermoelasticity to apply the fractional transfer of heat equation [8], along with a discussion of modified Fourier's law. The time-based fractional radial distribution

***Corresponding author.**
*E-mail address: navneetkumarlamba@gmail.com

This paper was recommended for publication in revised form by Editor-in-Chief Ahmet Selim Dalkilic

Published by Yıldız Technical University Press, İstanbul, Turkey

in a sphere was treated by Povstenko [9]. In the context of decoupling thermoelasticity, the heat transmission formula has a fractional component of time for an infinite medium, Povstenko [10] studied thermal loads.

Recently, numerous more prominent researchers have made major contributions [11–17] to the advancement of thermoelasticity with fractional techniques. Abouelregal et al. [18] utilized a memory-dependent variant of the heat transmission model and determined thermoelastic rotational nano-beams with changeable thermal characteristics. Using an integral transformation process, Lamba [19] presented the memory-based behaviour in a thick, solid thermoelastic cylindrical cylinder with an internal thermal source. Iyengar and Alwar [20] have given an overall solution for the induced stresses caused by a uniform transfer of temperature flow in a long rectangular plate. Iyengar and Chandrashekhara [21] have established the stress caused by temperature with boundary constraints. Chen [22] uses a direct power series method to tackle the linear issues associated with stress in a rectangular thin plate. Tanigawa and Komatsubara [23] established the thermal variation assessment in the two-dimensional plane stress situation and examined its intensity. Morimoto et al. [24] use the example of thermal buckling of an inhomogeneous plate with rectangular dimensions with heat input.

Kulkarni and Deshmukh [25] explored the problem based on the thermal analysis of a quasi-static plate of rectangular dimensions. Also, Deshmukh et al. [26-29] described the effect of thermal bending on the rectangle-shaped plate problem. A discussion of the thermoelastic phenomenon of a thin plate of rectangular dimensions caused by a partially dispersed thermal supply was carried out by Lamba and Khobragade [27]. Further, Lamba and Khobragade [28] explored various aspects related to the three-dimensional inverse modeling of the rectangular plate problem. Manthena et al. [30] analyse in detail the behaviour of heat and mechanical inhomogeneity in the case of a rectangular plate. They also carry out numerical calculations while taking into consideration the fluctuation in inhomogeneous characteristics. A rectangular-shaped plate with non-homogeneous material characteristics that generated heat was studied by Manthena et al. [31] to evaluate the heat distribution, movement, and stresses caused by temperature. Aleck [32] found an approximate explanation for the pressures produced by a uniform temperature change in a thin, camped, rectangular-shaped plate. Sedelnikov et al. [33] developed analytical methods for the study of a homogeneous plate that underwent a shock. Also, the fractional approach is adopted by some more authors in knowing the behaviour of solids as reflected in [34, 35]. Lamba and Deshmukh [36] studied the memory effect in a solid body of infinite length and successfully determined the temperature, displacement, and stress functions. Lamba et al. [37] discussed both space- and time-based fractional ordered behaviour in a finite-length layer under certain boundaries. Demirbas et al. [38] utilized the finite difference method to determine the thermo-mechanical behaviour of the plate for different compositional gradient exponents. Eslami [39] presented the development of the theory of thermoelasticity by considering solid plates.

Gunasekar et al. [40, 41] presented the transform approach for the solution of integro-differential equations. Using a basic fractional calculus method, Raghavendran et al. [42] investigated approaches to various families of fractional integro-differential equations

The present manuscript is prepared on the basis of the literature given in the book title "Thermal Stresses" by Noda et al. [43] and we modified this basic idea and prepared the mathematical modelling. No recent literature was studied by any researcher except the work done by one of the authors, Deshmukh et al. [29], by considering problem of circular plate with bending moments. The above work is based on only the classical heat conduction of a rectangular plate with a bending moment. Whereas in the present manuscript, we modified the classical heat conduction of the problem by introducing the fractional derivative in the heat transfer equation, which interpolates the classical heat conduction equation, and the impact of the retarded response is discussed successfully.

In this article, we have studied the heat transfer equations using fractional order theory and discussed the effects of thermal stresses with an additional heat source and thermal bending moments using fractional order theory. Till date, only studies have shown the thermal bending moment for classical heat conduction equations, whereas this paper, considered heat conduction containing a fractional order approach, which predicts the retarded response, and it also interpolates classical heat conduction equations. This kind of work has not been cited so far, which contributes to the development of thermoelasticity based on fractional analysis and is useful for various material structure designs under the influence of additional heat generation. This is our new and novel contribution to the field of thermoelasticity.

MODELLING OF FRACTIONAL THERMOELASTIC PROBLEM

Let's assume a rectangular plate with dimension $\{D: 0 < x < a, 0 < y < b, 0 < z < c\}$, which is maintained at a temperature $F(x, y, z)$ initially. All of the boundary constraints are maintained at absolute zero. In such cases, it is crucial to calculate the thermoelasticity in conjunction with a rectangular plate that is simply supported. The shape of a plate that is rectangular with a simple support is shown in Figure 1.

To better fit this problem to physical conditions, fractional derivatives of time order are used for the fluctuation of temperature, and an additional thermal source is also used in setting up the heat transfer equation. The rectangular plate's bending stiffness or thermal produced resultant moment are both factors in the fundamental equation of deflection. This type of modeling can play an important role

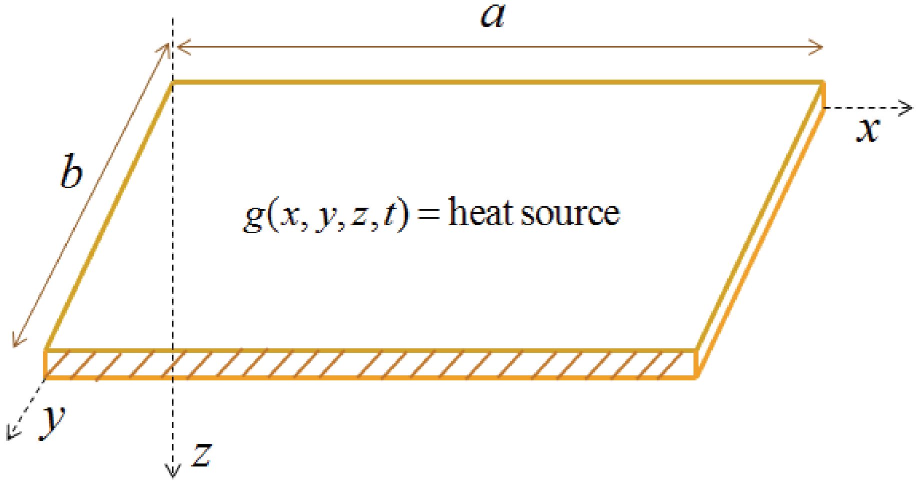

Figure 1. Geometrical design of rectangular-shaped plate with source of heat under fraction order theory.

in classifying materials based on fracture parameters and is capable of describing the actual behaviour of materials.

Governing Heat Transfer Equation

The fractional derivative-based modeling of heat conduction for homogeneous and isotropic rectangular-shaped solids with fractional order differential and heat generation is given by

$$\nabla^2 T + \frac{1}{k} g(x,y,z,t) = \frac{1}{A}\frac{\partial^\alpha T}{\partial t^\alpha}. \tag{1}$$

Subjected to the conditions

$$T(at\ all\ assumed\ boundaries) = 0. \tag{2}$$

$$T(t=0) = U(x,y,z), \quad 0 < \alpha \le 1 \tag{3}$$

$$\frac{\partial T(x,y,z,0)}{\partial t} = 0. \qquad 1 < \alpha \le 2 \tag{4}$$

where Tdenotes the function of temperature flow, A and k stands for the thermal conductivity and thermal diffusivity of the material of the plate respectively and $\alpha$is the fractional order parameter. Also $g(x, y, z, t)$ denotes the instantaneous point source of heat situated at any point inside the rectangular solid plate.

Since the thickness of the assumed plate is believed to be insignificant, one observes a rectangular plate with simple support that has had a thermal load applied $a \times b$ dimensions.

Bending Moments, Thermal Deflection and Thermal Stresses

Following [26, 29], the basic formula and related boundary circumstances in the Cartesian system of coordinates are

$$\nabla^2\nabla^2 w = \frac{-1}{(1-\nu)R}\nabla^2 M_T. \tag{5}$$

where

$$\nabla^2 = \frac{\partial^2}{\partial x^2} + \frac{\partial^2}{\partial y^2} + \frac{\partial^2}{\partial z^2}$$

with

$$w = 0, \frac{\partial^2 w}{\partial x^2} = \frac{-1}{(1-\nu)R} M_T, \text{ on } x = 0, x = a \tag{6}$$

and

$$w = 0, \frac{\partial^2 w}{\partial y^2} = \frac{-1}{(1-\nu)R} M_T, \text{ on } y = 0, y = b \tag{7}$$

where w and ν are notations denote the deflection and Poisson's ratio respectively.

The plate's bending stiffness and the consequent moment caused by the heat, respectively, are denoted by the letters R and M_T are defined as

$$M_T = a_t E \int_0^c Tzdz. \tag{8}$$

and

$$R = \frac{Eh^3}{12(1-\nu^2)}. \tag{9}$$

where a_t and E, respectively, represent the linear heat expansion coefficient and Young's modulus.

One focuses on the equilibrium condition in the x and y in-plate dimensions. Consequently, the in-plate resulting forces becomes

$$N_x = N_y = N_{xy} = 0. \tag{10}$$

The definition of the resultant moments per unit length of the plate reads as follows:

$$M_x = -R\left(\frac{\partial^2 w}{\partial x^2} + \nu \frac{\partial^2 w}{\partial y^2}\right) - \frac{1}{1-\nu} M_T, \tag{11}$$

$$M_y = -R\left(\frac{\partial^2 w}{\partial y^2} + \nu \frac{\partial^2 w}{\partial x^2}\right) - \frac{1}{1-\nu} M_T, \tag{12}$$

and

$$M_{xy} = (1-\nu) R \frac{\partial^2 w}{\partial x \partial y}. \tag{13}$$

The equations for moments' equilibrium about the x and y axes are

$$\frac{\partial M_x}{\partial x} + \frac{\partial M_{yx}}{\partial y} - Q_x = 0, \tag{14}$$

$$\frac{\partial M_y}{\partial y} - \frac{\partial M_{xy}}{\partial x} - Q_y = 0. \tag{15}$$

where the shearing forces are denoted by Q_x, Q_y.

The thermal stress elements are stated as [26] in terms of the resulting forces and resulting moments as

$$\sigma_{xx} = \frac{1}{c} N_x + \frac{12z}{c^3} M_x + \frac{1}{(1-\nu)}\left(\frac{1}{c} N_T + \frac{12z}{c^3} M_T - \alpha_t E T\right), \tag{16}$$

$$\sigma_{yy} = \frac{1}{c} N_y + \frac{12z}{c^3} M_y + \frac{1}{(1-\nu)}\left(\frac{1}{c} N_T + \frac{12z}{c^3} M_T - \alpha_t E T\right), \tag{17}$$

and

$$\sigma_{xy} = \frac{1}{c} N_{xy} - \frac{12z}{c^3} M_{xy}. \tag{18}$$

where the resultant force is

$$N_T = \alpha_t E \int_0^c T dz. \tag{19}$$

The deflection

$$w(x = a, y = b) = 0. \tag{20a}$$

the moments

$$M_x(x = a, y = b) = M_y(x = a, y = b) = 0. \tag{20b}$$

the shearing forces

$$Q_x = Q_y = 0. \tag{20c}$$

the thermal stresses

$$\sigma_{xx}(x = a, y = b) = \sigma_{yy}(x = a, y = b) = 0. \tag{20d}$$

The problem is mathematically formulated in Equations (1) through (20).

Analytical Approach to Solve a Mathematical Modeled Problem

The integral transformation method—which is covered in the subsection below—is used to get the solution to the heat transfer equation for rectangular-shaped solids with fractional order differential and heat generation.

Solution of Heat Transfer Equation

To obtain the desired temperature function, one constructs the "Triple Analytic Transformation" and its inverted formula.

$$\bar{T}(\phi_m, \theta_n, \psi_p, t) = \int_{x=0}^{a} \int_{y=0}^{b} \int_{z=0}^{c} S(\psi_p, z) S(\theta_n, y) S(\phi_m, x) T(x, y, z, t) dxdydz \tag{21}$$

$$T(x, y, z, t) = \sum_{p=1}^{\infty} \sum_{n=1}^{\infty} \sum_{m=1}^{\infty} S(\psi_p, z) S(\theta_n, y) S(\phi_m, x) \bar{T}(\psi_p, \theta_n, \phi_m, t) \tag{22}$$

where the kernels are $S(\phi_m, x)$, $S(\theta_n, y)$ and $S(\psi_p, z)$ are obtained and are defined as

$$S(\phi_m, x) = \sqrt{\frac{2}{a}} \sin \phi_m x \text{ where } \phi_m = \frac{m\pi}{a}, m = 1,2,3 \ldots \tag{23a}$$

$$S(\theta_n, y) = \sqrt{\frac{2}{b}} \sin \theta_n y \text{ where } \theta_n = \frac{n\pi}{b}, n = 1,2,3 \ldots \tag{23b}$$

$$S(\psi_p, z) = \sqrt{\frac{2}{c}} \sin \psi_p z \text{ where } \psi_p = \frac{p\pi}{c}, p = 1,2,3 \ldots \tag{23c}$$

Moreover, the transcendental equations

$$\sin \phi_m a = 0, \sin \theta_n b = 0, \sin \psi_p c = 0 \tag{24}$$

when the equations (1) to (4) are transformed using the triple integral transform described in (21), one obtains

$$\int_{x=0}^{a} \int_{y=0}^{b} \int_{z=0}^{c} S(\psi_p, z) S(\theta_n, y) S(\phi_m, x) (\nabla^2 T) dxdydz + \frac{\bar{g}(x,y,z,t)}{k} = \frac{1}{A} \frac{d^\alpha T}{dt^\alpha} \tag{25}$$

By employing the theorem known as Green's to solve the problem (25), one can derive an expression such as

$$\frac{d^\alpha \bar{T}}{dt^\alpha} + A\left({\phi_m}^2 + {\theta_n}^2 + {\psi_p}^2\right) \bar{T} = \frac{A}{k} \bar{g}(\psi_p, \theta_n, \phi_m, t) \tag{26}$$

with

$$\bar{T}(\psi_p, \theta_n, \phi_m, t) = \bar{U}(\psi_p, \theta_n, \phi_m) \text{ at } t = 0 \tag{27}$$

Solving the equation (26), one obtains

$$\bar{T}(\psi_p, \theta_n, \phi_m, t) = \frac{A}{k}\int_0^t \tau^{\alpha-1} E_{\alpha,\alpha}\left(-A\left({\phi_m}^2 + {\theta_n}^2 + {\psi_p}^2\right)t^\alpha\right) g(t-\tau)d\tau \tag{28}$$

where $E_{\alpha,\alpha}$ denotes for the Mittag Leffler function.

To obtain a mathematical expression of the temperature function, the triple integral transformation is inverted repeatedly by applying the inversion formula (22) to equation (27)

$$T(x,y,z,t) = \sum_{p=1}^{\infty}\sum_{n=1}^{\infty}\sum_{m=1}^{\infty} S(\psi_p, z) S(\theta_n, y) S(\phi_m, x) \left[\bar{U}(\phi_m, \theta_n, \psi_p) + \frac{A}{k}\int_0^t \tau^{\alpha-1} E_{\alpha,\alpha}\left(-A\left({\phi_m}^2, \theta_n^2, \psi_p^2\right)t^\alpha\right) g(t-\tau)d\tau\right] \tag{29}$$

Where,

$$\bar{U}(\phi_m, \theta_n, \psi_p) = \int_{x=0}^{a}\int_{y=0}^{b}\int_{z=0}^{c} S(\psi_p, z') S(\theta_n, y') S(\phi_m, x') F(x', y', z') dx' dy' dz'$$

Determination of Bending Moments, Thermal Deflection and Thermal Stresses

Using equation (29) in equations (8) and (19), one obtains the expression of the resultant moment and resultant forces as below:

$$M_T = AEc\sqrt{\frac{2}{c}}\sum_{p=1}^{\infty}\sum_{n=1}^{\infty}\sum_{m=1}^{\infty}\frac{(-1)^{p+1}}{\eta_p} S(\theta_n, y)\, S(\phi_m, x) \left\{\bar{U}(\phi_m, \theta_n, \psi_p) + \frac{A}{k}\int_0^t \tau^{\alpha-1}E_{\alpha,\alpha}\left[-A\left({\phi_m}^2, {\theta_n}^2, {\psi_p}^2\right)t^\alpha\right] g(t-\tau)d\tau\right\} \tag{30}$$

$$N_T = \alpha E\sqrt{\frac{2}{c}}\sum_{p=1}^{\infty}\sum_{n=1}^{\infty}\sum_{m=1}^{\infty}\frac{[(-1)^{p+1}+1]}{\eta_p} S(\theta_n, y)\, S(\phi_m, x) \left\{\bar{U}(\phi_m, \theta_n, \psi_p) + \frac{A}{k}\int_0^t \tau^{\alpha-1}E_{\alpha,\alpha}\left[-A\left({\phi_m}^2, {\theta_n}^2, {\psi_p}^2\right)t^\alpha\right] g(t-\tau)d\tau\right\} \tag{31}$$

Equations (30) and (31) represent the resultant moment and resultant forces respectively.

Utilizing equation (30) in (5) the expression of thermal deflection obtained as

$$w(x,y) = \frac{AEc}{(1-\nu)R}\sqrt{\frac{2}{c}}\sum_{p=1}^{\infty}\sum_{n=1}^{\infty}\sum_{m=1}^{\infty}\frac{(-1)^{p+1}}{\psi_p({\phi_m}^2)} S(\theta_n, y)\, S(\phi_m, x) \left\{\bar{U}(\phi_m, \theta_n, \psi_p) + \frac{A}{k}\int_0^t \tau^{\alpha-1}E_{\alpha,\alpha}\left[-A\left({\phi_m}^2, {\theta_n}^2, {\psi_p}^2\right)t^\alpha\right] g(t-\tau)d\tau\right\} \tag{32}$$

Using equations (30) and (32) in (11), (12) and (13), one obtains the resultant moments as,

$$M_x = -AEc\sqrt{\frac{2}{c}}\sum_{p=1}^{\infty}\sum_{n=1}^{\infty}\sum_{m=1}^{\infty}\frac{(-1)^{p+1}}{\psi_p}\left(\frac{{\theta_n}^2}{{\phi_m}^2+{\theta_n}^2}\right) S(\theta_n, y)\, S(\phi_m, x) \left\{\bar{U}(\phi_m, \theta_n, \psi_p) + \frac{A}{k}\int_0^t \tau^{\alpha-1}E_{\alpha,\alpha}\left[-A\left({\phi_m}^2, {\theta_n}^2, {\psi_p}^2\right)t^\alpha\right] g(t-\tau)d\tau\right\} \tag{33}$$

$$M_y = -AEc\sqrt{\frac{2}{c}}\sum_{p=1}^{\infty}\sum_{n=1}^{\infty}\sum_{m=1}^{\infty}\frac{(-1)^{p+1}}{\psi_p}\left(\frac{{\phi_m}^2}{{\phi_m}^2+{\theta_n}^2}\right) S(\theta_n, y)\, S(\phi_m, x) \left\{\bar{U}(\phi_m, \theta_n, \psi_p) + \frac{A}{k}\int_0^t \tau^{\alpha-1}E_{\alpha,\alpha}\left[-A\left({\phi_m}^2, {\theta_n}^2, {\psi_p}^2\right)t^\alpha\right] g(t-\tau)d\tau\right\} \tag{34}$$

$$M_{xy} = AEc\sqrt{\frac{2}{a}}\sqrt{\frac{2}{b}}\sqrt{\frac{2}{c}}\sum_{p=1}^{\infty}\sum_{n=1}^{\infty}\sum_{m=1}^{\infty}\frac{(-1)^{p+1}}{\psi_p}\left(\frac{\phi_m\theta_n}{{\phi_m}^2+{\theta_n}^2}\right)\cos\theta_n y \cos\phi_m x \left\{\bar{U}(\phi_m, \theta_n, \psi_p) + \frac{A}{k}\int_0^t \tau^{\alpha-1}E_{\alpha,\alpha}\left[-A\left({\phi_m}^2, {\theta_n}^2, {\psi_p}^2\right)t^\alpha\right] g(t-\tau)d\tau\right\} \tag{35}$$

Using equations (10),(29),(30),(31),(33),(34), and (35) in equations (16), (17), and (18), we get the thermal stress functions mathematically as

$$\begin{aligned}\sigma_{xx} = \frac{12z}{c^2}&\left(-AE\sqrt{\frac{2}{c}}\sum_{p=1}^{\infty}\sum_{n=1}^{\infty}\sum_{m=1}^{\infty}\frac{(-1)^{p+1}}{\eta_p}\left(\frac{{\theta_n}^2}{{\phi_m}^2+{\theta_n}^2}\right)S(\theta_n, y)S(\phi_m, x)\right)\\ &+\frac{1}{c(1-\nu)}\left(\frac{2\sqrt{2}AE}{\pi\sqrt{abc}}\sum_{p=1}^{\infty}\sum_{n=1}^{\infty}\sum_{m=1}^{\infty}\frac{[(-1)^{p+1}+1]}{p}\sin\theta_n y \sin\phi_m x\bar{U}(\psi_p, \theta_n, \phi_m)\right)\\ &+\frac{12z}{c^2(1-\nu)}\left(\frac{2\sqrt{2}AE}{\pi\sqrt{abc}}\sum_{p=1}^{\infty}\sum_{n=1}^{\infty}\sum_{m=1}^{\infty}\frac{(-1)^{p+1}}{p}\sin\theta_n y \sin\phi_m x\bar{U}(\psi_p, \theta_n, \phi_m)\right)\\ &-\frac{1}{(1-\nu)}\left(\frac{2\sqrt{2}AE}{\sqrt{abc}}\sum_{p=1}^{\infty}\sum_{n=1}^{\infty}\sum_{m=1}^{\infty}\sin\psi_p z \sin\theta_n y \sin\phi_m x\bar{U}(\psi_p, \theta_n, \phi_m)\right)\\ &\times\left\{\bar{U}(\phi_m, \theta_n, \psi_p) + \frac{A}{k}\int_0^t \tau^{\alpha-1}E_{\alpha,\alpha}\left[-A\left({\phi_m}^2, {\theta_n}^2, {\psi_p}^2\right)t^\alpha\right] g(t-\tau)d\tau\right\}\end{aligned} \tag{36}$$

$$\begin{aligned}\sigma_{yy} = \frac{12z}{c^2}&\left(-AE\sqrt{\frac{2}{c}}\sum_{p=1}^{\infty}\sum_{n=1}^{\infty}\sum_{m=1}^{\infty}\frac{(-1)^{p+1}}{\eta_p}\left(\frac{{\beta_m}^2}{{\beta_m}^2+{\upsilon_n}^2}\right)S(\theta_n, y)S(\phi_m, x)\right)\\ &+\frac{1}{c(1-\nu)}\left(\frac{2\sqrt{2}AE}{\pi\sqrt{abc}}\sum_{p=1}^{\infty}\sum_{n=1}^{\infty}\sum_{m=1}^{\infty}\frac{[(-1)^{p+1}+1]}{p}\sin\theta_n y \sin\phi_m x\bar{U}(\psi_p, \theta_n, \phi_m)\right)\\ &+\frac{12z}{c^2(1-\nu)}\left(\frac{2\sqrt{2}AE}{\pi\sqrt{abc}}\sum_{p=1}^{\infty}\sum_{n=1}^{\infty}\sum_{m=1}^{\infty}\frac{(-1)^{p+1}}{p}\sin\theta_n y \sin\phi_m x\bar{U}(\psi_p, \theta_n, \phi_m)\right)\\ &-\frac{1}{(1-\nu)}\left(\frac{2\sqrt{2}AE}{\sqrt{abc}}\sum_{p=1}^{\infty}\sum_{n=1}^{\infty}\sum_{m=1}^{\infty}\sin\psi_p z \sin\theta_n y \sin\phi_m x\bar{U}(\psi_p, \theta_n, \phi_m)\right)\\ &\left\{\bar{U}(\phi_m, \theta_n, \psi_p) + \frac{A}{k}\int_0^t \tau^{\alpha-1}E_{\alpha,\alpha}\left[-A\left({\phi_m}^2, {\theta_n}^2, {\psi_p}^2\right)t^\alpha\right] g(t-\tau)d\tau\right\}\end{aligned} \tag{37}$$

$$\sigma_{xy} = \frac{12z}{c^2}\left(-AE\sqrt{\frac{2}{a}}\sqrt{\frac{2}{b}}\sqrt{\frac{2}{c}}\sum_{m=1}^{\infty}\sum_{n=1}^{\infty}\sum_{p=1}^{\infty}\frac{(-1)^{p+1}}{\eta_p}\left(\frac{\phi_m\theta_n}{{\phi_m}^2+{\theta_n}^2}\right)\cos\theta_n y \cos\phi_m x\right) \left\{\bar{U}(\phi_m, \theta_n, \psi_p) + \frac{A}{k}\int_0^t \tau^{\alpha-1}E_{\alpha,\alpha}\left[-A\left({\phi_m}^2, {\theta_n}^2, {\psi_p}^2\right)t^\alpha\right] g(t-\tau)d\tau\right\} \tag{38}$$

Convergence Analysis

Numerical computations were made on different axes (x and y) to assess the impact of steady heat supply on the plate's extreme ends.

Consider

$$\lim_{m\to\infty}\phi_m = \lim_{n\to\infty}\theta_n = \lim_{p\to\infty}\psi_p = \infty$$
$$\lim_{m\to\infty} exp[-k\phi_m^2 t] = \lim_{n\to\infty} exp[-k\theta_n^2 t] = \lim_{p\to\infty} exp[-k\psi_p^2 t] = 0$$

The terms sine and cosine are also constrained. The required condition for convergence has been met, so it is simple to confirm that all of the aforementioned series are convergent by using D'Alembert's ratio test. Additionally, for large values of m, n, and p, the term in the calculation for temperature, deflection, and thermal stresses is minimal and converges to zero at infinity.

Numerical Computation

To make computations as simple as possible, we set the functions in dimensionless form as

Dimensionless form:

$$T^* = \frac{T}{T_0}, w^* = \frac{w}{a_t T_0 a}, x^* = \frac{x}{a}, y^* = \frac{y}{b}, z^* = \frac{z}{a}, \sigma_{ij}^* = \frac{\sigma_{ij}}{E a_t}, \tau = \frac{At}{a^2}$$

Material Properties

The computational analysis has been done for a plate with a rectangular shape made entirely of copper-based material properties [26, 29].

Thermal conductivity, $A = 386Wm^{-1}k^{-1}$
Thermal diffusivity, $k = 112.34 \times 10^{-6}m^2s^{-1}$
Density, $\rho = 8954kgm^{-3}$
Specific heat, $c_p = 383Jkg^{-1}k^{-1}$
Poisson ratio, $\nu = 0.35$
Coefficient of linear thermal expansion, $a_t = 16.5 \times 10^{-6}k^{-1}$
Lames constant, $\mu = 26.67$

Dimensions

The following dimensions are set for numerical computations:
Length of a rectangular plate, $a = 2m$
Breadth of a rectangular plate, $b = 1m$
Height of rectangular plate, $c = 0.5m$

GRAPHICAL ILLUSTRATION AND DISCUSSION

Arbitrary establishing heat supply $T = T_0$ and instantaneous point heating source of strength g_0 located at location (x_0, y_0, z_0) inside the material spontaneously releases heat at the time $T = \tau$.

$$g(x, y, z, t) = g_0\delta(x - x_0)\delta(y - y_0)\delta(z - z_0)\delta(t - t_0)$$

Below Figures 2 to 5 represent the graphical plotting temperature distribution, deflection variation, and stress dispersion along axial directions for different fractional parameters.

The value of y is fixed at $0.5m$ respectively for plotting along x axis, similarly the value of x is fixed at $1m$ for plotting along $y$axis and for the plotting along x and y axis, the value of z and time $t$are fixed at $0.25m$ and 0.5 respectively.

Figure 2(a) and 2(b) display the display of dimensionless temperature T^* and dimensionless defection distribution ω^*

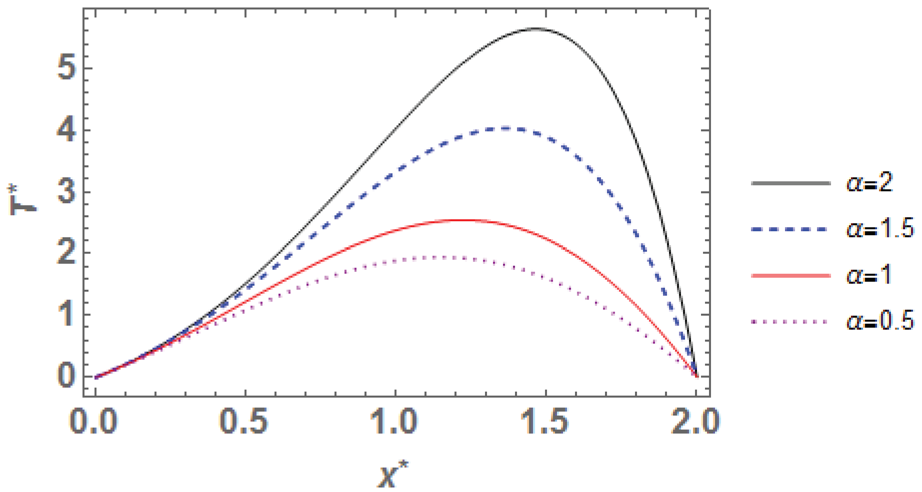

Figure 2(a). Influence of fractional parameters on temperature behaviour along the x^* axis.

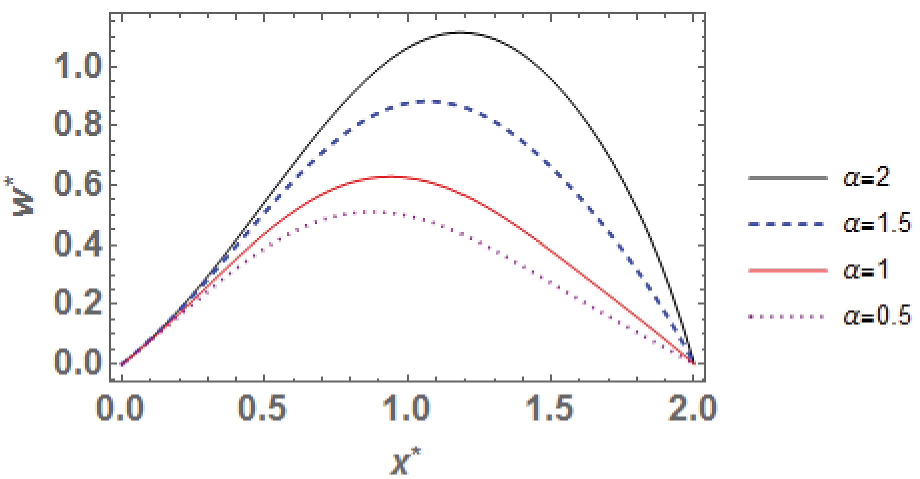

Figure 2(b). Influence of fractional parameters on deflection behaviour along the x^* axis.

along dimensionless x^* axis for various values of fractional parameters $\alpha = 0.5, 1, 1.5, 2$. It can be seen in both plots that temperature and defect rise in the x^* direction from the initial edge to about the midway and decrease towards the extreme edge. Additionally, it is evident that the largest temperature distribution and deflection are found in the middle, it could be caused by an effect of the source point of heat. The speed of thermal signal transmission is discovered to be directly related to the variation of the fraction-order parameter α, and temperature and deflection adopt a uniform pattern for various values of fractional parameters α. Furthermore, deflection ω^*at points $x^* = 0$ and $x^* = 2$ is zero, this agrees with the necessary boundary criteria stated in equation (6).

For various values of the fractions parameters $\alpha = 0.5$, 1, 1.5, 2, Figure 3(a) and 3(b) demonstrate the fluctuation of without dimension temperature $T^*$and defection distribution ω^* along dimensionless y^* axis. The rate of thermal signal propagation is shown to be directly related to the parameters denoting the fraction-order differentiation in both plots. Additionally, when one moves into the y^* direction from the initial edge towards the middle, the temperature and deflection rise and then fall as one approaches the extreme edge. Further, slight discrimination in both temperature and deflection distribution is noted as compared to distribution in x^*direction. Also, deflection ω^* is zero at $y^* = 0$ and $y^* = 1$ which matches with the prescribed boundary condition defined in equation (7).

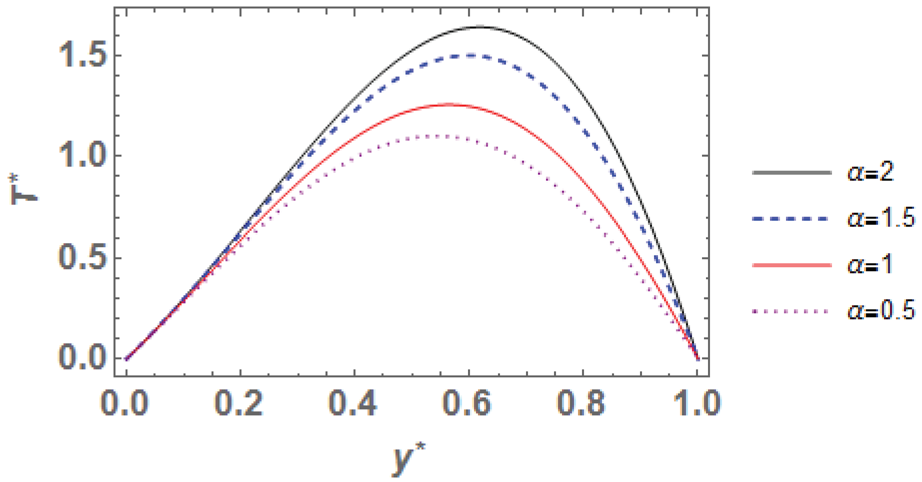

Figure 3(a). Influence of fractional parameters on temperature behaviour along the y^* axis.

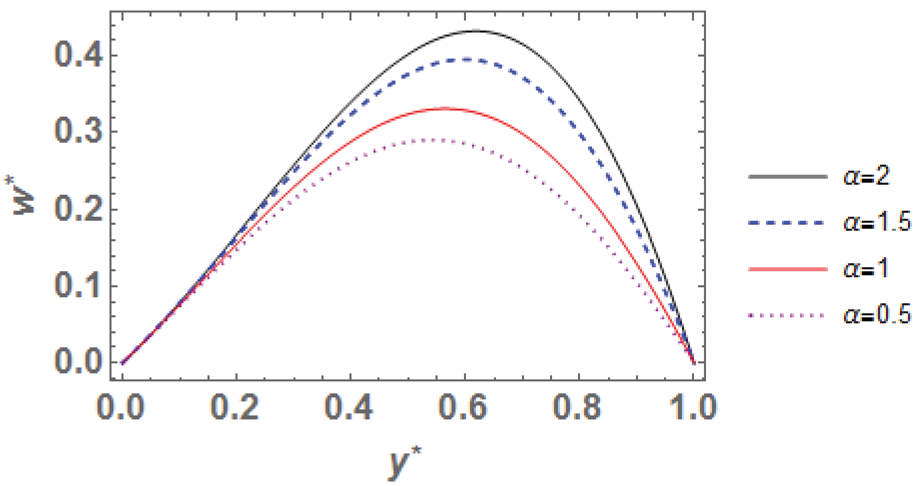

Figure 3(b). Influence of fractional parameters on deflection behaviour along the y^* axis.

Figure 4(a), 4(b) and 4(c) demonstrate the graphical view of dimensionless stress distributions σ_{xx}^*, σ_{yy}^*, σ_{xy}^*, respectively along x^* for various values of fractional

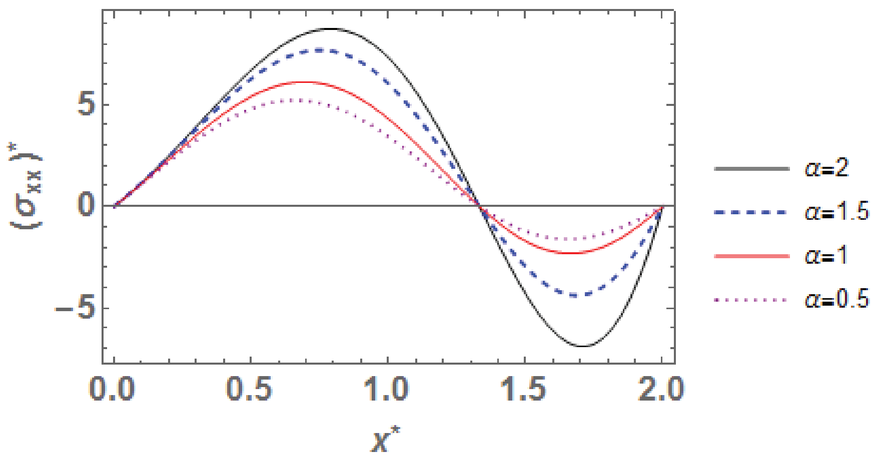

Figure 4(a). Influence of fractional parameters on stress σ_{xx}^* behaviour along the x^* axis.

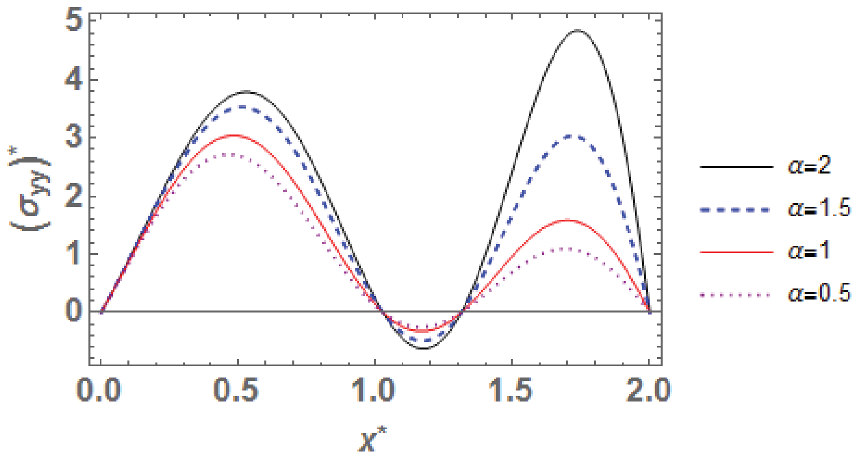

Figure 4(b). Influence of fractional parameters on stress σ_{yy}^* behaviour along the x^* axis.

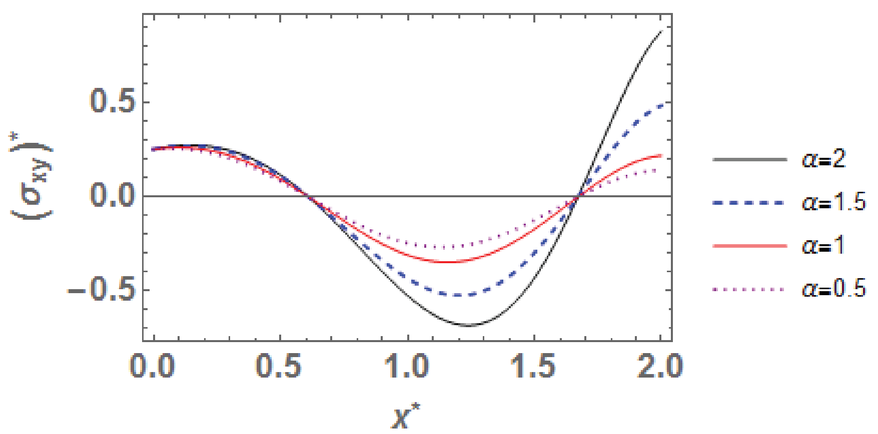

Figure 4(c). Influence of fractional parameters on stress σ_{xy}^* behaviour along the x^* axis.

parameters $\alpha = 0.5$, 1, 1.5,2. The following observations are noted from graphical plotting:

(a) Stress function $\sigma_{xx}{}^*$ grows in the vicinity $0 \le x^* \le 0.74$, $1.5 \le x^* \le 2$ and falls in the vicinity $0.76 \le x^* \le 1.49$, whereas maximum distribution in $\sigma_{xx}{}^*$ is attained at $x^* = 0.75$.

(b) Stress distribution for $\sigma_{yy}{}^*$ grows in the vicinity $0 \le x^* \le 0.5$, $1.2 \le x^* \le 1.74$ and falls in the vicinity $0.5 \le x^* \le 1.19$,$1.76 \le x^* \le 2$ maximum distribution in $\sigma_{yy}{}^*$ is attained at $x^* = 1.75$.

(c) Stress distribution $\sigma_{xy}{}^*$ falls in the vicinity $0 \le x^* \le 1.24$ and grow in the vicinity $1.25 \le x^* \le 2$maximum distribution in $\sigma_{xy}{}^*$ is attained at $x^* = 1.5$.

(d) All the stress functions $\sigma_{xx}{}^*$, $\sigma_{yy}{}^*$ and $\sigma_{xy}{}^*$ varies propagation to different values of fractional parameters α.

(e) Stresses $\sigma_{xx}{}^*$, $\sigma_{yy}{}^*$ are compressive throughout the curve while $\sigma_{xy}{}^*$ is tensile at the extreme edge.

(f) Stress function $\sigma_{xx}{}^*$ becomes zero for $x^* = 2$ which matches the mathematical condition defined in equation (20c).

Figure 5(a), 5(b) and 5(c) demonstrate the graphical view of dimensionless stress distributions $\sigma_{xx}{}^*$, $\sigma_{yy}{}^*$, $\sigma_{xy}{}^*$ respectively along y^* for various fractional parameters $\alpha = 0.5$, 1, 1.5,2. The following observations are noted from graphical plotting:

(a) Stress function $\sigma_{xx}{}^*$ grows in the range $0 \le y^* \le 0.29$, $0.8 \le y^* \le 1$ and falls in the vicinity $0.31 \le y^* \le 0.79$, whereas maximum distribution in $\sigma_{xx}{}^*$ is attained at $y^* = 0.3$.

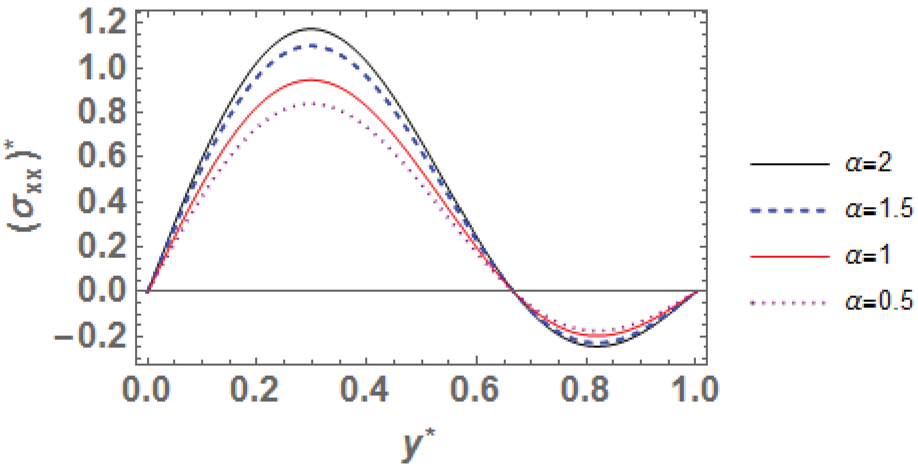

Figure 5(a). Influence of fractional parameters on stress $\sigma_{xx}{}^*$ behaviour along the y^* axis.

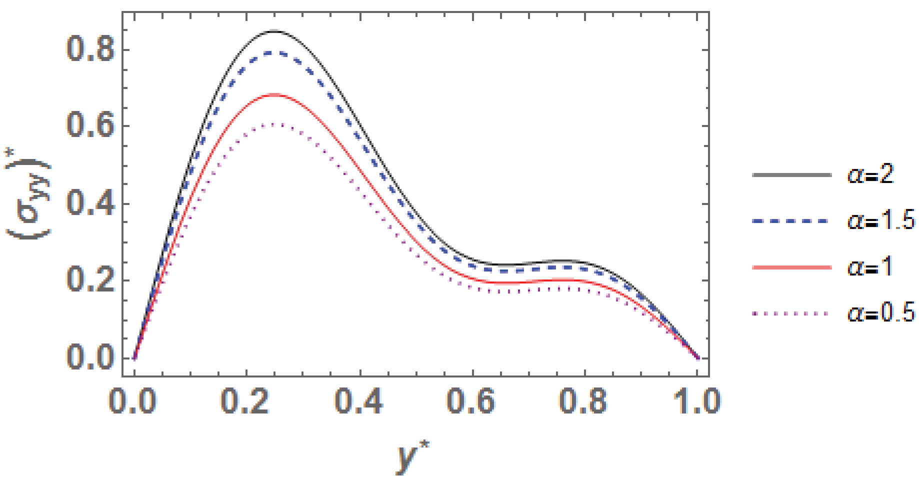

Figure 5(b). Influence of fractional parameters on stress $\sigma_{yy}{}^*$ behaviour along the y^* axis.

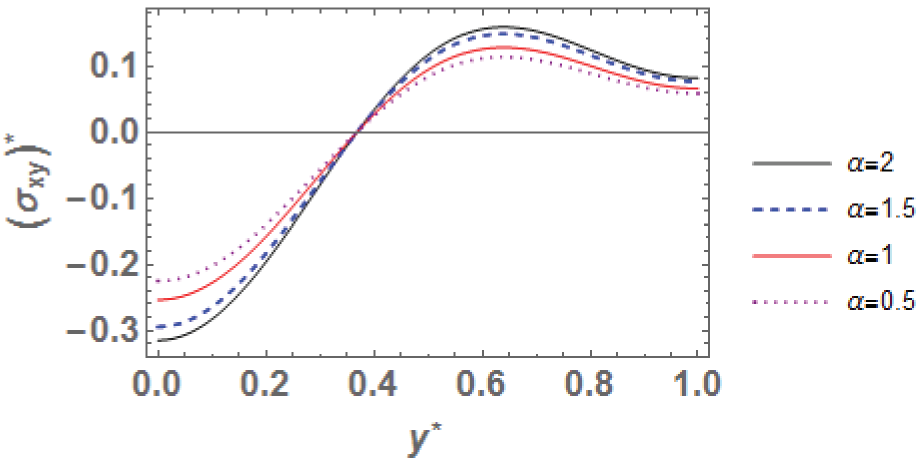

Figure 5(c). Influence of fractional parameters on stress $\sigma_{xy}{}^*$ behaviour along the y^* axis.

(b) Stress distribution for $\sigma_{yy}{}^*$ starts increasing from the initial edge and reaches its peak at $y^* = 0.2$ and then starts gradually decreasing towards the extreme edge.
(c) Stress distribution for $\sigma_{xy}{}^*$ starts increasing from the initial edge and reaches its peak at $y^* = 0.75$ and then slightly decreases towards the extreme edge.
(d) Significant impact of fractional parameters α is observed in stress functions $\sigma_{xx}{}^*$, $\sigma_{yy}{}^*$ and $\sigma_{xy}{}^*$ along y^* axis.
(e) Stresses $\sigma_{xx}{}^*$, $\sigma_{yy}{}^*$ are compressive throughout the curve while $\sigma_{xy}{}^*$ is tensile at the initial and extreme edges.
(f) Stress function $\sigma_{yy}{}^*$ becomes zero for $y^* = 1$ which matches the mathematical condition defined in equation (20c).

RESULTS AND DISCUSSION

Based on numerical computation, the following significant outcome summaries were obtained:

- The deflection on the boundary at $x = a$ and $y = b$ is seen to be insignificant since the moments and shearing forces in the x and y directions are negligible, which fulfilled the uniqueness and existence of the problem.
- The thermal stresses $\sigma_{xx} = \sigma_{yy} = 0$ at $x = a$, $y = b$, which shows that they are traction-free.
- Numerical representation shows that higher thermal response is observed for a higher value of fractional order parameter.
- Due to the initial constant heat input from internal heat generation, significant stresses and deflections develop in a rectangular region.
- Both the resulting components of stress and the shear stress components vary greatly from the initial edge to the outermost edge of the rectangular plate and conform to the specified mathematical boundary conditions.
- The variation in the temperature, deflection, and stress functions is confined to a restricted range, and no variation is observed excluding this range. This phenomenon reflects the fact that waves propagate with finite speed.
- The creation of novel structural materials for physical processing is dependent on the wave propagation rate since changing values of the fractional parameters have an impact on it. The result can be seen schematically.
- It can be observed that the resultant moments caused by heat and forces are strongly influenced by the response of the weak, medium, and superconductivity, which have a direct influence on the characteristics of the thermal variation in temperature, deflection, and stress distribution.
- The effects of temperature, deflection, and stress functions for different fraction order parameters show the weak, medium, and superconductivity. Also, for fractional parameters $\alpha = 1$ and $\alpha = 2$ heat transfer interpolates the diffusion and wave equation and then effects on bending moments and stresses are shown in the figures, which represent the limiting case.

CONCLUSION

An analytical approach is used to effectively analyse the thermoelastic behaviour for a simply supported thin rectangular plate that has a thermal bending moment and a heat source. Here, the concept of resultant forces and moments per unit length of the plate is used to know the exact thermal response of the rectangular plate under the fractional theory, additionally, by excluding the in-plane resultant forces and accounting for the thermal bending moments, the stress components are assessed. A rectangular copper plate was numerically calculated, and the results of thermal change, including temperature and deflection along different axes based on different fractional parameters, are effectively presented and discussed.

Finally, the authors study fractional order theory to investigate the thermal effect of the time fractional derivative on a rectangular plate, which deals with the memory effect and interpolates the classical heat conduction equation for a rectangular plate. Also due to fractional order theory effectiveness of heat and elastic waves inputting $\alpha = 0$, $\alpha = 1$, $\alpha = 2$ it predicts the classical heat conduction equations i.e. Helmholtz, diffusion, and wave equation. Also noting for $\alpha = 1$, it is the limiting case of the study by Deshmukh et al. [29].

FUTURE SCOPE OF THE RESULTS

It may be helpful to build various thermo-mechanical structures with bending moments and subjected to additional heat sources by using the researched inhomogeneous boundary value issue of a rectangular plate under fractional thermoelasticity, which is essential for capturing the real behaviour of materials. Also, this work might potentially be extended to investigate the thermal bending moment by introducing the concept of memory-dependent derivatives to investigate the behaviour of materials in practical circumstances.

ACKNOWLEDGMENT

The authors are very thankful to respected Prof. Dr. Ahmet Selim Dalkılıç, Editor-in-Chief, for their valuable guidance to improve the manuscript, as well as to respected reviewers for their valuable comments for improving the quality of research work.

AUTHORSHIP CONTRIBUTIONS

Authors equally contributed to this work.

DATA AVAILABILITY STATEMENT

The authors confirm that the data that supports the findings of this study are available within the article. Raw data that support the finding of this study are available from the corresponding author, upon reasonable request.

CONFLICT OF INTEREST

The author declared no potential conflicts of interest with respect to the research, authorship, and/or publication of this article.

ETHICS

There are no ethical issues with the publication of this manuscript.

REFERENCES

[1] Podlubny I. Fractional Differential Equations. Academic Press, San Diego, 1999.
[2] Atanackovic TM, Pilipovic S, Stankovic B, Zorica D. Fractional Calculus with Applications in Mechanics. Vibrations and Diffusion Processes. Wiley-ISTE, London, 2014. [CrossRef]
[3] Herrmann R. Fractional Calculus. An Introduction for Physicists, 2nd edn. World Scientific, Singapore, 2014. [CrossRef]
[4] Magin RL. Fractional Calculus in Bioengineering. Begell House Publishers, Connecticut, 2006.
[5] Mainardi F. Fractional Calculus and Waves in Linear Viscoelasticity. An Introduction to Mathematical Models. Imperial College Press, London, 2010. [CrossRef]
[6] West BJ, Bologna M, Grigolini P. Physics of Fractals Operators. Springer, New York, 2003. [CrossRef]
[7] Zaslavsky GM. Hamiltonian Chaos and Fractional Dynamics. Oxford University Press, New York, 2005. [CrossRef]
[8] Povstenko YZ. Fractional Heat Conduction Equation and Associated Thermal Stresses. J Therm Stresses 2004;28:83–102. [CrossRef]
[9] Povstenko YZ. Time-fractional radial diffusion in a sphere. Nonlinear Dyn 2008;53:55–65. [CrossRef]
[10] Povstenko YZ. Fractional radial heat conduction in an infinite medium with a cylindrical cavity and associated thermal stresses. Mech Res Commun 2010;37:436–440. [CrossRef]
[11] Sherief H, El-Said A, Abd El-Latief A. Fractional order theory of thermoelasticity. Int J Solids Struct 2010;47:269–275. [CrossRef]
[12] Jiang X, Xu M. The time fractional heat conduction equation in the general orthogonal curvilinear coordinate and the cylindrical coordinate systems. Physica A 2010;389:3368–3374. [CrossRef]
[13] Ezzat MA. Theory of fractional order in generalized thermoelectric MHD. Appl Math Model 2011;35:4965–4978. [CrossRef]
[14] Ezzat MA, El-Karamany AS, El-Bary A, Fayik MA. Fractional calculus in one-dimensional isotropic thermo-viscoelasticity. C R Mech 2013;341:553–566. [CrossRef]
[15] Povstenko YZ. Thermal stresses in a long cylinder under Gaussian-distributed heating in the framework of fractional thermoelasticity. Math Model Comput 2015;2:77–87. [CrossRef]
[16] Caputo M, Fabrizio M. A new definition of fractional derivative without singular kernel. Progr Fract Differ Appl 2015;1:73–85.
[17] Raslan WE. Application of fractional order theory of thermoelasticity in a thick plate under axisymmetric temperature distribution. J Therm Stresses 2015;38:733–743. [CrossRef]
[18] Abouelregal AE, Atta D, Sedighi HM. Vibrational behaviour of thermoelastic rotating nanobeams with variable thermal properties based on memory-dependent derivative of heat conduction model. Arch Appl Mech 2023;93:197–220. [CrossRef]

[19] Lamba N. Impact of Memory-dependent Response of a Thermoelastic Thick Solid Cylinder. J Appl Comput Mech 2023;9:1135–1143.
[20] Iyengar KT, Sundara RS, Alwar RS. Thermal stresses in a long rectangular plate constrained at one of the shorter edges. Int J Mech Sci 1962;4:485–490. [CrossRef]
[21] Iyengar KT, Sundara RS, Chandrashekhara K. Thermal stresses in rectangular plates. Appl Sci Res 1996;15:141–160. [CrossRef]
[22] Chen PYP. Transient thermal stresses in a rectangular plate due to non-uniform heat transfer coefficients. J Therm Stresses 1998;11:115–125. [CrossRef]
[23] Tanigawa Y, Komatsubara Y. Thermal stress analysis of a rectangular plate and its thermal stress intensity factor for compressive stress field. J Therm Stresses 1997;20:517–542. [CrossRef]
[24] Morimoto T, Tanigawa Y, Kawamura R. Thermal buckling analysis of inhomogeneous rectangular plate due to uniform heat supply. J Therm Stresses 2003;26:1151–1170. [CrossRef]
[25] Kulkarni VS, Deshmukh KC. A brief note on quasi-static thermal stresses in a rectangular plate. Far East J Appl Math 2007;26:349–360.
[26] Deshmukh KC, Khandait MV, Warbhe SD, Kulkarni VS. Thermal stresses in a simply supported plate with thermal bending moments. Int J Appl Math Mech 2010;6:1–12.
[27] Lamba NK, Khobragade NW. Thermoelastic problem of a thin rectangular plate due to partially distributed heat supply. Int J Appl Math Mech 2012;8:1–11.
[28] Lamba NK, Khobragade NW. Integral transform methods for inverse problem of heat conduction with known boundary of a thin rectangular object and its stresses. J Therm Sci 2012;21:459–465. [CrossRef]
[29] Deshmukh KC, Khandait MV, Kumar R. Thermal stresses in a simply supported plate with thermal bending moments with heat sources. Mater Phys Mech 2014;21:135–146.
[30] Manthena VR, Lamba NK, Kedar GD. Transient thermoelastic problem of a nonhomogeneous rectangular plate. J Therm Stresses 2017;40:627–640. [CrossRef]
[31] Manthena VR, Lamba N, Kedar GD. Thermoelastic analysis of a rectangular plate with nonhomogeneous material properties and internal heat source. J Solid Mech 2018;10:200–215.
[32] Aleck BJ. Thermal stresses in a rectangular plate clamped along an edge. ASME J Appl Mech 2021;16:118–122. [CrossRef]
[33] Sedelnikov AV, Orlov DI, Serdakova V, Nikolaeva AS. Investigation of the stress-strain state of a rectangular plate after a temperature shock. Mathematics 2023;11:638. [CrossRef]
[34] Bikram J, Kedar G. Study of Thermoelastic behaviour, Efficiency and Effectiveness of Rectangular Fin with Fractional Order Energy Balance Equation. Int J Thermodyn 2021;24:216–225. [CrossRef]
[35] Gaikwad K, Khavale S. Fractional Order Transient Thermoelastic Stress Analysis of a Thin Circular Sector Disk. Int J Thermodyn 2022;25:1–8. [CrossRef]
[36] Lamba NK, Deshmukh KC. Memory dependent response in an infinitely long thermoelastic solid circular cylinder. PNRPU Mech Bull 2024;1:5–12. [CrossRef]
[37] Lamba N, Verma J, Deshmukh KC (R2028). A Brief Note on Space Time Fractional Order Thermoelastic Response in a Layer. Appl Appl Math: An Int J (AAM) 2023;18:1.
[38] Demirbas MD, Apalak MK, Ekici R. Determination of three-dimensional thermo-mechanical behaviour of bidirectional functionally graded rectangular plates with the theory of elasticity. Mech Adv Mater Struct 2024;31:1534–1562. [CrossRef]
[39] Eslami MR. Thermal Stresses in Plates. In: Thermal Stresses in Plates and Shells. Cham: Springer Nature Switzerland; 2024:43–143. [CrossRef]
[40] Gunasekar T, Raghavendran P, Santra SS, Majumder D, Baleanu D, Balasundaram H. Application of Laplace transform to solve fractional integro-differential equations. J Math Comput Sci-JM 2024;33:225–237. [CrossRef]
[41] Gunasekar T, Raghavendran P. The Mohand Transform Approach to Fractional Integro-Differential Equations. J Comput Anal Appl 2024;33:358–371. [CrossRef]
[42] Raghavendran P, Gunasekar Th, Balasundaram H, Santra SS, Majumder D, Baleanu D. Solving fractional integro-differential equations by Aboodh transform. J Math Comput Sci-JM 2024;32:229–240. [CrossRef]
[43] Noda N, Hetnarski RB, Tanigawa Y. Thermal Stresses, 2nd Edition. Taylor Francis, New York, 2003.